ORGANOMETALLICS

Article

pubs.acs.org/Organometallics

# Cyclometalated *Z*-Selective Ruthenium Metathesis Catalysts with Modified N-Chelating Groups

Myles B. Herbert,[†,§] Benjamin A. Suslick,[†,§] Peng Liu,[‡] Lufeng Zou,[‡] Peter K. Dornan,[†] K. N. Houk,*[,‡] and Robert H. Grubbs*[,†]

[†]Arnold and Mabel Beckman Laboratory of Chemical Synthesis, Division of Chemistry and Chemical Engineering, California Institute of Technology, Pasadena, California 91125, United States

[‡]Department of Chemistry and Biochemistry, University of California, Los Angeles, California 90095, United States

Supporting Information

**ABSTRACT:** In order to design improved ruthenium catalysts for *Z*-selective olefin metathesis reactions, four cyclometalated catalysts with new chelated architectures were synthesized, structurally characterized, and tested in metathesis assays. The mechanism of formation of each was explored using DFT calculations. Of note, two complexes are derived from activation of a tertiary C−H bond, and one features a four-membered chelating architecture. In addition, two dipivalate complexes that did not undergo further C−H activation were isolated and studied to elucidate information about the factors affecting cyclometalation.

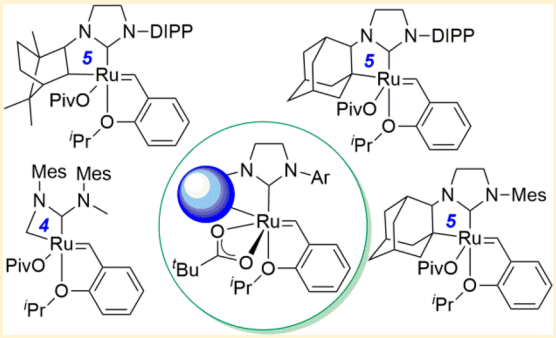


## INTRODUCTION

Since its discovery in the 1950s, olefin metathesis has become a premier reaction for the construction of carbon−carbon double bonds.[1] The continued development of well-defined transition metal alkylidene catalysts has allowed metathesis to become highly prevalent in a wide variety of fields, including chemical biology,[2] materials science,[3] and green chemistry.[4] Controlling stereoselectivity in cross-metathesis (CM) reactions has long been a goal of research, as there is a pressing need to develop reliable routes to stereopure internal olefin products. Since the reaction is typically performed under thermodynamic control and traditional catalysts generally favor formation of the more stable *E*-isomer, the discovery and development of catalysts capable of preferentially producing the Z-olefin isomer was highly desired. The laboratories of Schrock and Hoveyda provided the first examples of *Z*-selective catalysts with monoaryloxide pyrrolidine (MAP) complexes of molybdenum and tungsten.[5]

More recently, our group has developed a class of *Z*-selective ruthenium-based catalysts that contain a cyclometalated N-heterocyclic carbene (NHC) ligand derived from C−H activation of an *N*-1-adamantyl substituent (Scheme 1).[6,7] The treatment of ruthenium dichloride complexes with an excess of a metal pivalate causes the exchange of the chloride ligands for pivalates, leading to the formation of a dipivalate-substituted complex. This species can then rapidly undergo a carboxylate-assisted C−H bond activation to yield the desired cyclometalated complex along with one equivalent of pivalic acid.[6] Thus far, no stable dipivalate-substituted ruthenium alkylidene complexes have been reported. Complexes that contain one chloride and one pivalate ligand, however, have been independently prepared and do not undergo C−H activation even upon heating.[8] These studies suggest that C−H activation occurs only from the dipivalate complex and not from the monochloride, monopivalate complex. Silver(I) pivalate (AgOPiv) was originally used as a ligand exchange and C−H activation reagent, though it was later found to induce the decomposition of the desired cyclometalated catalysts.[9] For some ruthenium complexes, the salt metathesis steps are slow and the resulting cyclometalated species decompose prior to isolation. We thus desired to find conditions using a less reactive metal pivalate to promote the ligand exchange. It was discovered that exposing certain ruthenium alkylidene complexes to sodium pivalate (NaOPiv) in a 1:1 mixture of MeOH and THF led to clean formation of the desired cyclometalated catalysts without accompanying decomposition.[10,11]

With this mild method in hand and with the aid of DFT calculations,[12] we were able to develop a family of ruthenium

**Scheme 1. Salt Metathesis and Carboxylate Assisted C−H Activation To Produce Cyclometalated Catalyst 2**

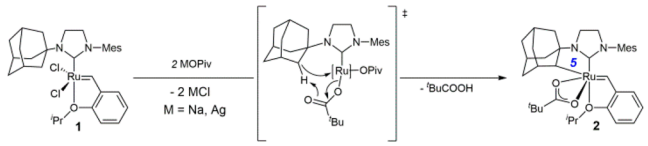


**Received:** March 5, 2015




DOI: 10.1021/acs.organomet.5b00185
*Organometallics* XXXX, XXX, XXX−XXX

catalysts with five-membered, *N*-1-adamantyl chelates that have exhibited remarkably high *Z*-selectivity and activity (Figure 1).

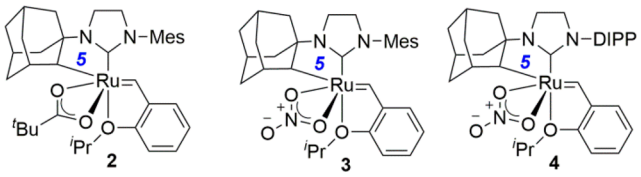


**Figure 1.** Prominent cyclometalated ruthenium catalysts for *Z*-selective olefin metathesis.

Our first highly *Z*-selective catalyst (**2**) features a pivalate X-type ligand and an *N*-mesityl group as the nonchelated NHC substituent.[13] This complex was able to catalyze the homodimerization of terminal olefins with ∼90% selectivity for the *Z*-olefin at 1 mol % catalyst loading. It was subsequently found that substitution of the pivalate ligand of **2** with a nitrate ligand led to formation of catalyst **3**, which now exhibited ∼95% *Z*-selectivity in homodimerization reactions.[14] When the nonchelating *N*-aryl NHC substituent was changed to an *N*-2,6-diisopropylphenyl (DIPP) group, the selectivity increased further, as catalyst **4** exhibited >98% selectivity in analogous homodimerization reactions.[10] Catalysts **3** and **4** also proved to be more active than **2** and could be used at catalyst loadings as low as 0.01 mol %. These three cyclometalated catalysts have proven effective in more complicated cross metathesis,[15] macrocyclic ring-closing metathesis (mRCM),[16] asymmetric ring-opening cross metathesis (AROCM),[17] ethenolysis,[18] and ring-opening metathesis polymerization (ROMP)[19] reactions.

Although significant advancements in the design of cyclometalated complexes have been made, one area that has yet to be thoroughly investigated is the effect of the N-chelating group on activity and selectivity. Five catalysts bearing chelating groups other than an *N*-1-adamantyl group have been reported by our group and are depicted in Figure 2. Catalyst **5** features a

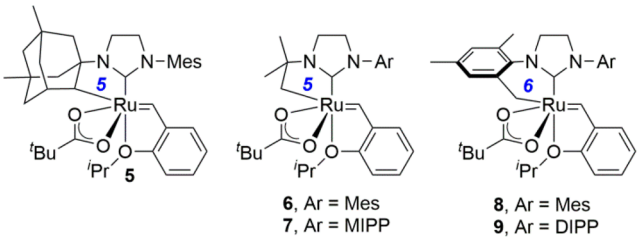


**Figure 2.** Previously reported catalysts bearing modified *N*-chelating groups. MIPP = 2-methyl-6-isopropylphenyl.

modified *N*-1-adamantyl group substituted with two bridgehead methyl groups and exhibits similar activity to catalyst **2**,[10] while catalysts **6** and **7** contain *N*-$^t$Bu chelates and exhibit no CM reactivity.[19b] Alternatively, catalysts **8** and **9** bear six-membered chelates and exhibit significantly reduced *Z*-selectivity in CM reactions.[8,13a] In this report, several new chelating architectures were synthesized in an effort to understand how chelate size and geometry affect both catalyst activity and selectivity. The barriers to C–H activation of each species were determined by DFT calculations, which aided in the prediction of which isomer would preferentially form when the chelating substituent contained multiple, accessible C–H bonds. The metathesis activity of these new cyclometalated catalysts was subsequently probed in standard terminal olefin homodimerization reactions. Additionally, two stable dipivalate complexes were isolated and studied for the development of improved cyclometalated catalysts.

## RESULTS AND DISCUSSION

**Synthesis of New Cyclometalated Architectures.** Due to the unpredictable stability of cyclometalated architectures, we first sought to screen various ruthenium dichloride alkylidene complexes to determine whether a stable cyclometalated species could form after a carboxylate-assisted C–H bond insertion event. A number of complexes were prepared with varying N-substituents. These complexes were subsequently exposed to a metal pivalate to determine if they could form a stable chelating ruthenium–carbon bond in the presence of an alkylidene, which was monitored using $^1$H NMR spectroscopy. Ten equivalents of NaOPiv were added to a solution of each complex in a 1:1 mixture of $CD_3OD$ and THF-$d_8$. With species that were able to form a stable complex, the starting material was readily converted to a cyclometalated species with concurrent generation of pivalic acid. Alternatively, with some species, a dipivalate complex resulting from salt metathesis of the starting material was observed before C–H activation occurred. If pivalic acid was generated with disappearance of the starting material dichloride complex or the analogous dicarboxylate adduct, and formation of a ruthenium hydride was observed, the complex was deemed unstable and not relevant for further study.

We first attempted to form a cyclometalated complex with a five-membered chelate derived from activation of the *N*-bornyl substituent of previously reported complex **10** (Scheme 2).

**Scheme 2. C–H Activation To Form Cyclometalated Complex 11**

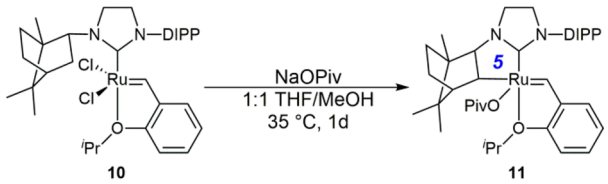


This carbocyclic group is markedly different in terms of structure and connectivity when compared to the previously reported *N*-1-adamantyl group. An *N*-DIPP group was chosen as the nonchelating substituent because it imparts improved activity and selectivity to this family of catalysts (*vide supra*). *N*-Bornyl complex **10** was treated with NaOPiv and formed the depicted cyclometalated complex according to two-dimensional NMR analysis (see Supporting Information). Despite containing multiple accessible C–H bonds, only one complex was stably formed. In order to explain the experimentally observed formation of product **11**, DFT calculations were performed.

Our previous mechanistic and computational studies indicated that the carboxylate-assisted C–H activation of the ruthenium dipivalate to form the *N*-1-adamantyl cyclometalated complex **2** occurs via a concerted metalation–deprotonation (CMD) mechanism.[20a,b] In the C–H activation transition state, the deprotonating pivalate adopts a pseudoapical geometry, displacing the aryl ether chelate. On the basis of this mechanism, we calculated the C–H activation pathways involving different C–H bonds of the *N*-bornyl group in the dipivalate-substituted complex **12** (Figure 3). The calculations were performed at the same level of theory in our recent


DOI: 10.1021/acs.organomet.5b00185
*Organometallics* XXXX, XXX, XXX–XXX

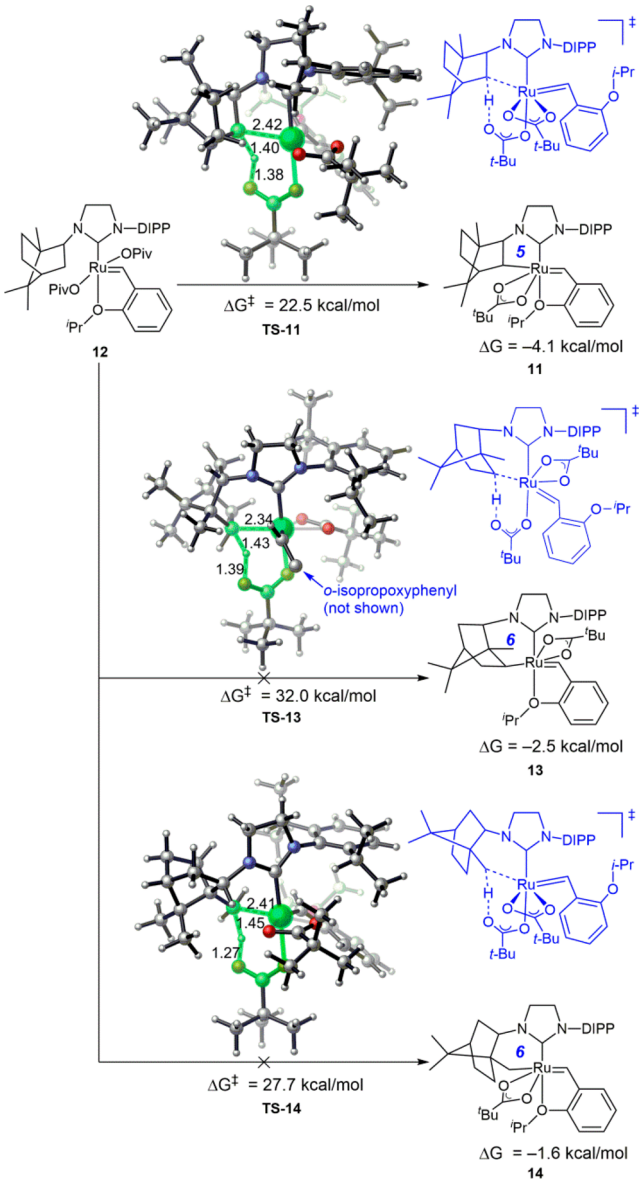


**Figure 3.** Transition states of C–H bond activation at different sites of dipivalate complex **12** and corresponding cyclometalated products. The Gibbs free energies are with respect to the dipivalate complex **12**.

computational studies of ruthenium metathesis catalysts.[6] Geometries were optimized with B3LYP[21] and the LANL2DZ basis set for Ru and 6-31G(d) for other atoms. Single-point energies were calculated with M06[22] and the SDD basis set for Ru and 6-311+G(d,p) for other atoms. The SMD[23] solvation model in THF solvent was employed in the single-point energy calculations. All calculations were performed with Gaussian 09.[24]

The computed Gibbs free energies of the rate- and selectivity-determining C–H activation transition states and the corresponding cyclometalated products are shown in Figure 3. Formation of the five-membered chelate (**11**) is predicted to be favored both kinetically and thermodynamically. The corresponding six-membered chelating complexes (**13** and **14**) are 2–3 kcal/mol less stable than **11**, and the barriers for C–H activation to form these complexes are more than 5 kcal/mol higher than that to form the five-membered chelate. These calculations are consistent with the experimental results that only the five-membered cyclometalated **11** complex is formed. The DFT calculations have allowed us to predict which isomer of a cyclometalated catalyst will preferentially form based on the relative barriers of C–H activation.[25]

Cyclometalated complexes derived from C–H activation of *N*-2-adamantyl NHC substituents were next investigated to elucidate the effect of a subtle change in the connectivity of the N-chelating group. The *N*-1-adamantyl group of dichloride complex **1** is unique in that the carbon atom that undergoes C–H activation sits quite close to the ruthenium center (2.80 Å) (Figure 4).[13a] The resulting cyclometalated complex (**2**) is

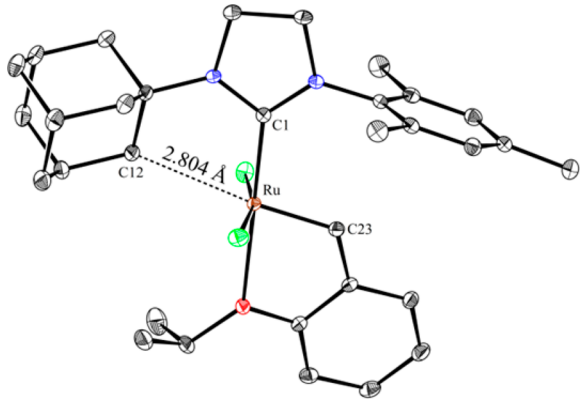


**Figure 4.** Previously reported crystal structure of dichloride complex **1**. Displacement ellipsoids are drawn at 50% probability. For clarity, hydrogen atoms have been omitted. Selected bond lengths (Å) for **1**: C1–Ru: 1.99, C23–Ru: 1.84; distance between C12 and Ru: 2.80.

seemingly less susceptible to insertion of the chelating ruthenium–carbon bond into the alkylidene and subsequent decomposition. Unlike the *N*-1-adamantyl-substituted complex **1** however, the solid-state structure of the *N*-2-adamantyl dichloride complex **15** does not feature any carbon atoms in close proximity to the ruthenium center (Figure 5). Nevertheless, complexes **15** and **17**, bearing an *N*-Mes and *N*-DIPP group, respectively, were exposed to NaOPiv and formed stable complexes **16** and **18** (Scheme 3). Single crystals of both were grown and the structures were determined by X-ray crystallography (Figures 6 and 7). These structures are derived from activation of a tertiary C–H bond to form a five-

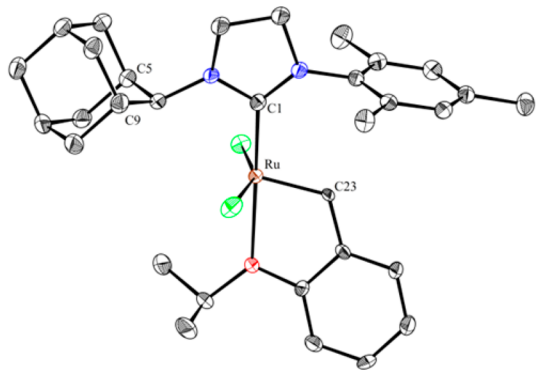


**Figure 5.** Crystal structure of ruthenium dichloride complex **15**. Displacement ellipsoids are drawn at 50% probability. For clarity, hydrogen atoms have been omitted. Selected bond lengths (Å) for **15**: C1–Ru: 1.97, C23–Ru: 1.84; distance between C5 and Ru: 3.99; distance between C9 and Ru: 4.28.



DOI: 10.1021/acs.organomet.5b00185
*Organometallics* XXXX, XXX, XXX–XXX

**Scheme 3. C−H Activation To Form Cyclometalated Complexes 16 and 18**

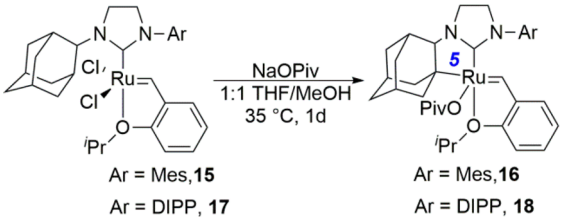


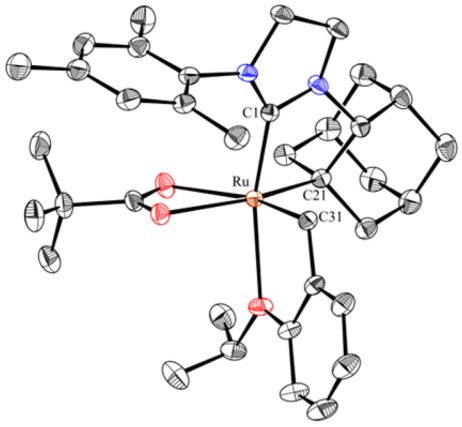


**Figure 6.** X-ray crystal structure of cyclometalated complex **16**. Displacement ellipsoids are drawn at 50% probability. For clarity, hydrogen atoms have been omitted. Selected bond lengths (Å) for **16**: C1−Ru: 1.95, C21−Ru: 2.08, C31−Ru: 1.85.

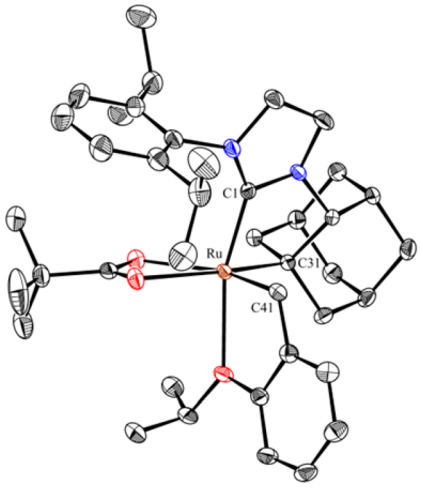


**Figure 7.** X-ray crystal structure of complex **18**. Displacement ellipsoids are drawn at 50% probability. For clarity, hydrogen atoms have been omitted. Selected bond lengths (Å) for **18**: C1−Ru: 1.95, C31−Ru: 2.08, C41−Ru: 1.85.

membered chelating architecture. DFT calculations were performed and revealed that the barriers of C−H activation to form **16** and **18** are 28.8 and 28.2 kcal/mol, respectively. These barriers are about 5 kcal/mol higher than those for the activation of the less hindered methylene C−H bonds to form the five-membered chelates **2** and **11** and are closer to those for six-membered chelates such as complex **8**.

Finally, we sought to determine if a previously reported ruthenium alkylidene complex (**19**) bearing an acyclic diamino carbene ligand could undergo cyclometalation (Scheme 4).[26]

**Scheme 4. C−H Activation To Form Cyclometalated Complex 20**

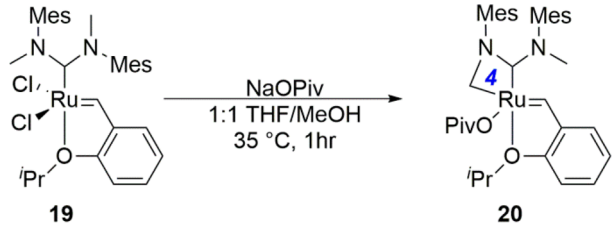


We initially thought that C−H activation of the *N*-methyl group would be unfavorable due to formation of a strained four-membered chelate, and therefore C−H activation would occur on the *N*-mesityl group to form a six-membered chelate. In the reported crystal structure of ruthenium dichloride complex **19**, however, the *N*-methyl group sits close to the ruthenium center (2.83 Å), while the *N*-mesityl *ortho*-methyl group is much farther away (Figure 8). Similarly to the *N*-1-

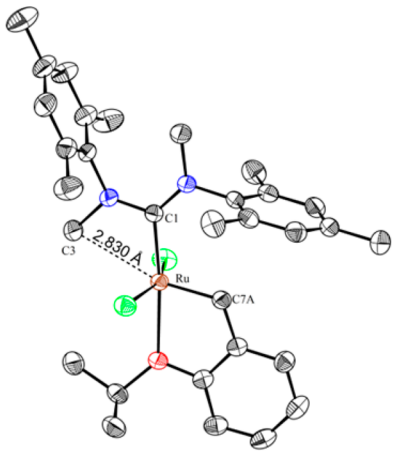


**Figure 8.** Previously reported crystal structure of dichloride complex **19**. Displacement ellipsoids are drawn at 50% probability. For clarity, hydrogen atoms have been omitted. Selected bond lengths (Å) and angles (deg) for **19**: C1−Ru: 2.01, C7A−Ru: 1.84, N−C1−N: 119.6; distance between C3 and Ru: 2.83.[26a]

adamantyl complex **1**, upon treatment with NaOPiv, the C−H bond proximal to the ruthenium center, on the *N*-methyl group in this case, underwent C−H activation to form complex **20**, containing a stable four-membered chelate. The structure was confirmed by X-ray crystallographic analysis (Figure 9). It seems that the flexibility of the acyclic carbene ligand allows the smaller and more strained chelate to form as a stable complex.

DFT calculations indicated that formation of the four-membered chelate from **19** has a much lower activation barrier and leads to a more stable cyclometalated complex compared to formation of the six-membered chelate via activation of the mesityl C−H bond (Figure 10). This selectivity is attributed to two effects. First, the greater N−C−N angle of the acyclic diamino carbene promotes formation of the four-membered chelate. The N−C−N angle increases from 117° in **21** to 124° in **TS-20** and 125° in **20** in the four-membered pathway, while it remains unchanged in the corresponding six-membered chelated structures (Figure 10). Additionally, in the transition state to form the planar four-membered chelate (**TS-20**), the C−H bond being deprotonated is oriented toward the bottom-bound carboxylate (see Figure 11 for a Newman projection


DOI: 10.1021/acs.organomet.5b00185
*Organometallics* XXXX, XXX, XXX−XXX

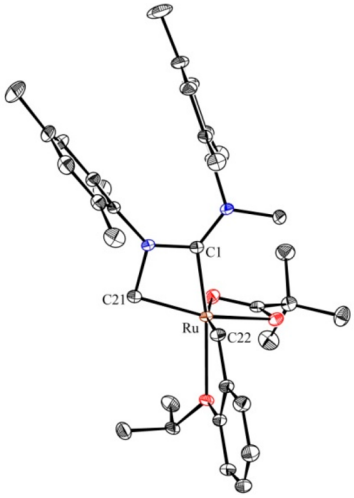


**Figure 9.** X-ray crystal structure of complex **20**. Displacement ellipsoids are drawn at 50% probability. For clarity, hydrogen atoms have been omitted. Selected bond lengths (Å) and angles (deg) for **20**: C1−Ru: 1.96, C21−Ru: 2.07, C22−Ru: 1.85, N−C1−N: 124.7.

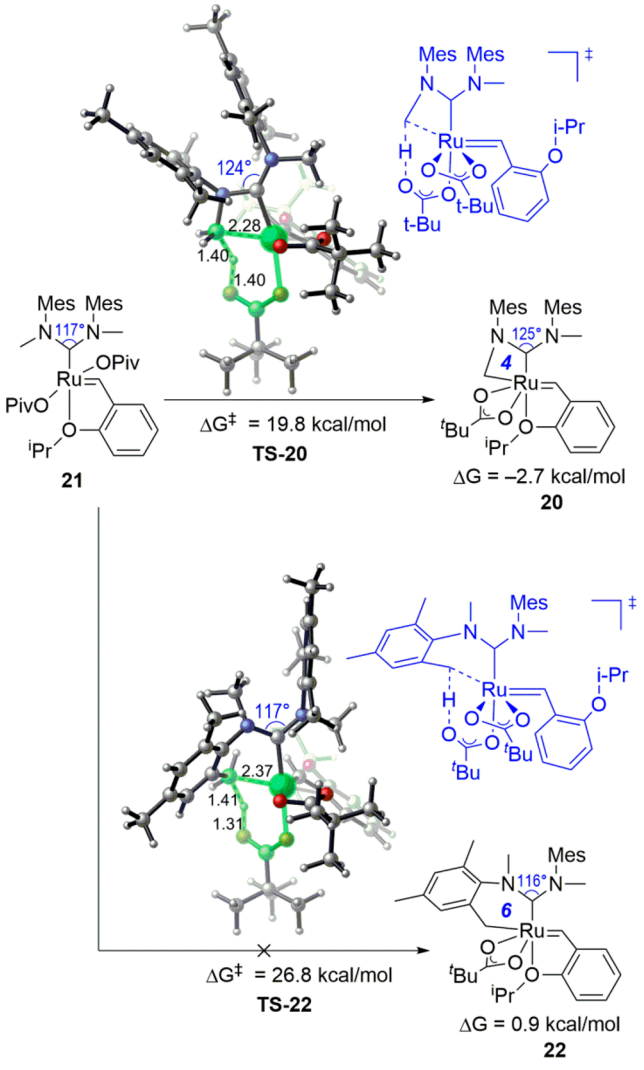


**Figure 10.** Transition states of C−H bond activation at different sites of dipivalate complex **21** and corresponding cyclometalated products. The Gibbs free energies are with respect to the dipivalate complex **21**.

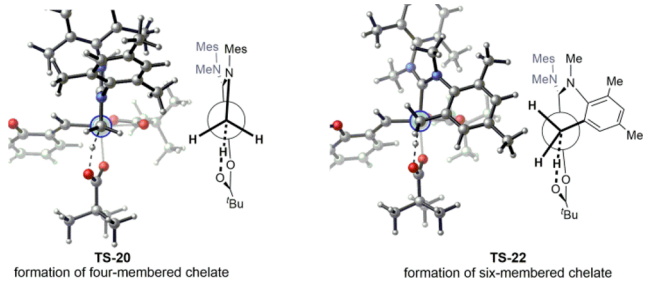


**Figure 11.** Newman projections along the forming Ru−C bond in transition states **TS-20** and **TS-22**.

along the forming Ru−C bond). In contrast, to form a puckered six-membered chelate in **TS-22**, significant distortion of the cleaving C−H bond is required to approach the bottom-bound carboxylate (Figure 11).

It has been shown experimentally that formation of planar (four- or five-membered) chelates is often more favorable than formation of puckered six-membered chelates. This selectivity trend is supported by the computed C−H activation barriers for various ruthenium NHC complexes shown in Table 1. Formation of smaller-ring chelates via activation of primary and secondary C−H bonds (entries 1−3) is predicted to be facile and always more favorable than forming a six-membered chelate with either *N*-mesityl or *N*-bornyl groups. Notably, formation of the sterically hindered five-membered chelates **16** and **18** (entries 4 and 5) requires higher barriers, which are still comparable to those for six-membered chelates resulting from activation of sterically more accessible primary or secondary C−H bonds (entry 6).

**Metathesis Activity and Selectivity of New Cyclometalated Catalysts.** The metathesis activities of the stable cyclometalated ruthenium complexes were evaluated using standard terminal olefin homodimerization reactions of allylbenzene (**24**), 4-penten-1-ol (**25**), and methyl-10-undecenoate (**26**).[13b] Allylbenzene is easily isomerized to *β*-methylstyrene by catalyst decomposition products. As such, it can act as an indicator of the stability of the active catalyst based on the ratio of isomerized product to the desired homocoupled product. 4-Penten-1-ol was chosen as a substrate because the homodimerized product undergoes undesired and rapid *Z* to *E* isomerization with previously reported *Z*-selective catalysts, and we had hoped we could find new cyclometalated complexes that would be improved in this regard. Discovery of new catalysts that maintain high *Z*-selectivity at high conversions is desired. Finally, methyl-10-undecenoate contains a functional group that is far removed from the olefin and does not typically undergo undesired side-reactions, making it a good test of the inherent metathesis reactivity of a catalyst.

Cyclometalated catalysts **11**, **16**, and **18** exhibited generally high *Z*-selectivity at early reaction times in the homodimerization assays tested, providing >75% of the *Z*-olefin product in most cases (Table 2). Unfortunately, these catalysts produced a significant amount of undesired olefin walking product in allylbenzene and 4-pentenol homodimerization assays. Additionally, for all substrates, but especially 4-pentenol, *Z* to *E* isomerization occurred readily.[27] Catalyst **20**, bearing a four-membered chelate, was metathesis inactive in all of the assays tested. This is not surprising, however, given that this catalyst contains the highly strained four-membered chelate, likely leading to facile decomposition.[9]



DOI: 10.1021/acs.organomet.5b00185
*Organometallics* XXXX, XXX, XXX−XXX

**Table 1. Computed Activation Barriers of C−H Activation To Form Four-, Five-, and Six-Membered Chelates**

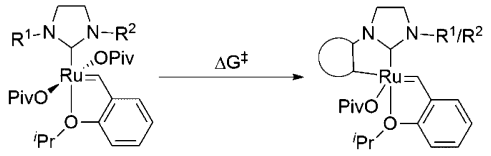


| entry | starting compound | $R^1$ | $R^2$ | product / $\Delta G^{\ddagger}$ (kcal/mol) |
|---|---|---|---|---|
| 1[a] | **1** | 1-Ada | Mes | 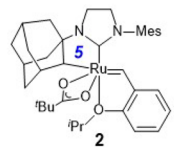 **2** (23.5); 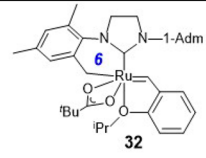 **32** (27.7) |
| 2[b] | **10** | bornyl | DIPP | 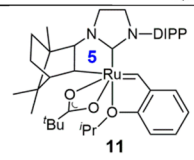 **11** (22.5); 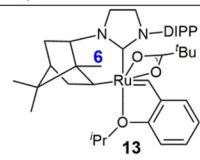 **13** (32.0); 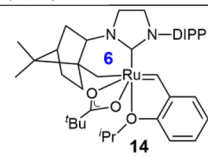 **14** (27.7) |
| 3[c] | **19** | 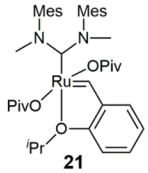 **21** | | 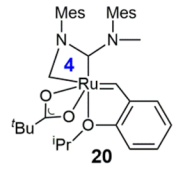 **20** (19.8); 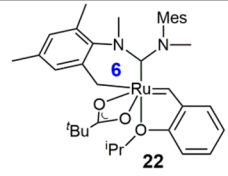 **22** (26.8) |
| 4 | **15** | 2-Ada | Mes | 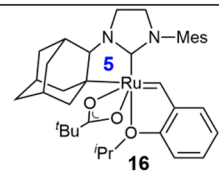 **16** (28.8) |
| 5 | **17** | 2-Ada | DIPP | 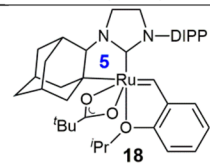 **18** (28.2) |
| 6[a] | **23** | Mes | Mes | 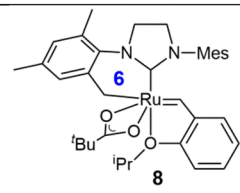 **8** (25.6) |
| 7 | **27** | 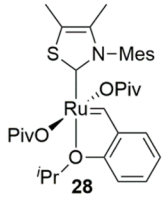 **28** | | 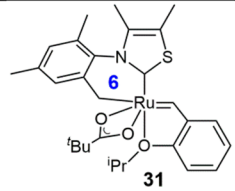 **31** (35.4) |

[a]See ref 6. [b]See Figure 3. [c]See Figure 10.

Catalysts **11** and **18**, bearing bulky *N*-DIPP groups, emerged as the best catalysts of those tested in terms of *Z*-selectivity. For allylbenzene and methyl-10-undecenoate homodimerization reactions, the *Z*-selectivity was generally >95% at early reaction



DOI: 10.1021/acs.organomet.5b00185
*Organometallics* XXXX, XXX, XXX−XXX

**Table 2. Homodimerization of Allylbenzene (24), 4-Penten-1-ol (25), and Methyl-10-undecenoate (26)**

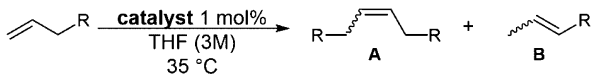


R = Ph (**24**), $(CH_2)_2OH$ (**25**), $(CH_2)_7CO_2Me$ (**26**)

| substrate | catalyst | time (h) | conv (%) | %Z-A | A/B |
|---|---|---|---|---|---|
| **24** | **11** | 1 | 54 | >95 | 2.7 |
| | | 2 | 86 | >95 | 1.0 |
| | | 4 | >95 | 90 | 0.8 |
| | **16** | 1 | 19 | 95 | 1.9 |
| | | 2 | 34 | 94 | 0.7 |
| | | 4 | 86 | 79 | 0.2 |
| | **18** | 1 | 10 | >95 | 2.1 |
| | | 2 | 16 | >95 | 1.0 |
| | | 4 | 31 | >95 | 0.6 |
| **25** | **11** | 1 | >95 | 74 | 3.4 |
| | | 2 | >95 | 63 | 2.6 |
| | | 4 | >95 | 55 | 2.2 |
| | **16** | 1 | 94 | 58 | 4.5 |
| | | 2 | >95 | 54 | 3.1 |
| | | 4 | >95 | 52 | 2.4 |
| | **18** | 1 | 31 | 83 | 3.8 |
| | | 2 | 82 | 88 | 1.6 |
| | | 4 | >95 | 81 | 1.4 |
| **26** | **11** | 1 | 83 | >95 | N/A |
| | | 2 | 92 | 93 | N/A |
| | | 4 | >95 | 74 | N/A |
| | **16** | 1 | 31 | 51 | N/A |
| | | 2 | 63 | 30 | N/A |
| | | 4 | 91 | 21 | N/A |
| | **18** | 1 | 19 | 93 | N/A |
| | | 2 | 28 | 90 | N/A |
| | | 4 | 39 | 75 | N/A |

times and did not fall below 74% after 4 h. *N*-Bornyl cyclometalated catalyst **11** proved to be slightly more active than *N*-2-adamantyl cyclometalated catalyst **18**, generally reaching higher conversions for all substrates. Catalyst **16**, bearing an *N*-2-adamantyl chelate and *N*-mesityl group, was inherently less *Z*-selective in the allylbenzene and methyl-10-undecenoate homodimerization reactions and exhibited more rapid *Z*-degradation. As expected, the 4-penten-1-ol homodimerization reactions exhibited significant *Z*/*E* isomerization for catalysts **11**, **16**, and **18** even after 1 h. Current efforts are aimed at understanding the complex and nuanced factors affecting *Z*-content degradation processes and will be reported in due time. Overall, these catalysts still showed reduced *Z*-selectivity, higher *Z*/*E* isomerization, and increased olefin walking compared to *N*-1-adamantyl chelated catalysts **2**–**4**. Thus, we believe that the *N*-1-adamantyl substituent is an ideal chelating group. Due to the unsatisfactory activity and selectivity of these newly reported catalysts, further catalyst development and optimization were not carried out.

**Isolation of Dipivalate Complexes.** During our investigations into forming new chelating architectures, we were able to isolate stable dipivalate complexes that unexpectedly did not undergo C–H activation; prior to this work, no ruthenium alkylidene dipivalate complexes had been reported. Since it has been shown that C–H activation occurs from dipivalate intermediates, studying these isolable complexes could provide important insight into why certain N-groups can be activated while others cannot. As previously mentioned, monochloride, monocarboxylate adducts have been independently prepared and do not undergo C–H activation even upon heating.[8]

We originally intended to C–H activate the benzylic carbon of an *N*-mesityl group of thiazole NHC-substituted **27** to form a six-membered chelating complex similar to complexes **8** and **9**.[28] However, a stable dipivalate-substituted complex (**28**) was formed instead, and even upon heating, C–H activation did not occur (Scheme 5). An X-ray crystal structure of **28** was

**Scheme 5. Salt Metathesis Reaction To Form Dipivalate Complex 28**

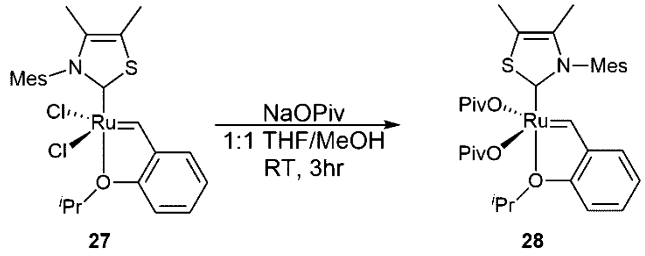


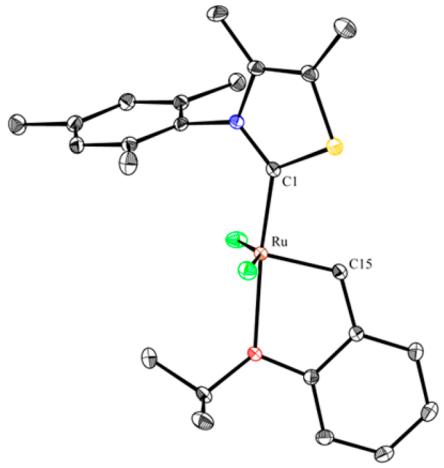


**Figure 12.** Crystal structure of complex **27**. Displacement ellipsoids are drawn at 50% probability. For clarity, hydrogen atoms have been omitted. Selected bond lengths (Å) for **27**: C1–Ru: 1.95, C15–Ru: 1.83.[28]

obtained and provided insight into why this complex did not undergo C–H activation (Figure 13). In the crystal structure of the starting complex **27**, the *N*-mesityl group resides over the chloride X-type ligands (Figure 12). In the structure of **28**, however, the NHC has rotated such that the *N*-mesityl group resides over the ruthenium alkylidene, most likely due to the increased steric bulk of the pivalate X-type ligands. As a result, the distance between the pivalate ligands and the *ortho*-methyl group of the *N*-mesityl substituent is too large to undergo a carboxylate-assisted activation event. The structure also features one monodentate pivalate ligand and one bidentate pivalate ligand. DFT calculations revealed that the barrier to C–H activation of this dipivalate complex was prohibitively high at 35.4 kcal/mol (Table 1, entry 7). This is in line with the high barriers to form six-membered chelates. In addition, replacing one of the *N*-mesityl groups with a S atom diminishes the steric strain in the dipivalate complex and thus leads to an even higher barrier than the cyclometalation of the *N*,*N*′-dimesityl NHC complex **23**. The agreement between computed and



DOI: 10.1021/acs.organomet.5b00185
*Organometallics* XXXX, XXX, XXX–XXX

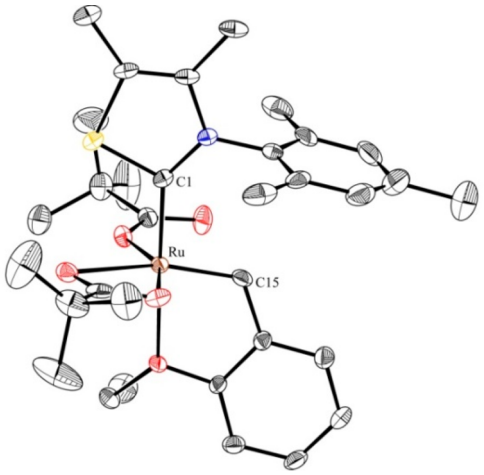


**Figure 13.** X-ray crystal structure of complex **28**. Displacement ellipsoids are drawn at 50% probability. For clarity, hydrogen atoms have been omitted. Selected bond lengths (Å) for **28**: C1−Ru: 1.97, C15−Ru: 1.84.

experimentally observed reactivities indicates that it is now becoming possible to predict whether a cyclometalated architecture can be formed by investigating the barriers of C−H activation of the corresponding dipivalate complex.

Similarly, when complex **29**, bearing an *N*-myrtanyl group, was treated with NaOPiv, dipivalate complex **30** was formed; however no C−H activation occurred even upon heating (Scheme 6). Unfortunately we were unable to obtain a crystal

**Scheme 6. Salt Metathesis Reaction To Form Dipivalate Complex 30**

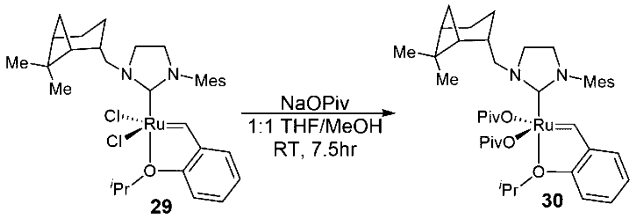


structure of the dipivalate complex; however instead we were able to obtain a crystal structure of the dichloride starting complex **29** (Figure 14). The methylene linker of this N-substituent seemingly gives the group added flexibility, allowing it to rotate away from the ruthenium center. Substitution of the chlorides with the bulky pivalates would likely increase the steric bulk of the congested ruthenium center and further push the *N*-myrtanyl group away, preventing C−H activation from occurring. It is also possible that the NHC ligand would rotate away from the pivalate-substituted metal center similar to what was observed for complex **28**. The information gained from the isolation and characterization of dipivalate-substituted complexes **28** and **30** will be important for the future design of more stable and improved *Z*-selective olefin metathesis catalysts.

## CONCLUSIONS

Four new cyclometalated ruthenium alkylidene complexes were synthesized, and the mechanism of their formation was investigated using DFT calculations. The use of a milder salt metathesis and C−H activation reagent, NaOPiv, has allowed

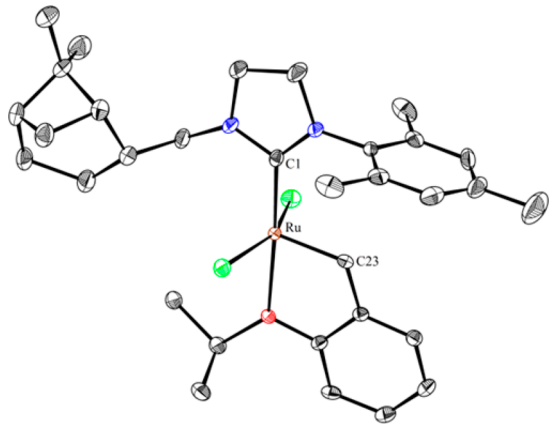


**Figure 14.** X-ray crystal structure of dichloride complex **29**. Displacement ellipsoids are drawn at 50% probability. For clarity, hydrogen atoms have been omitted. Selected bond lengths (Å) for **29**: C1−Ru: 1.98, C23−Ru: 1.83.

for the preparation of previously not accessible catalysts with chelating N-substituents other than *N*-1-adamantyl. New complexes containing multiple potential sites for C−H activation and tertiary C−H bonds were explored. Using DFT calculations, we were able to correctly predict which isomer of a cyclometalated complex will form by comparing the relative barriers of C−H activation. Formation of planar four- and five-membered chelates is found to be more favorable than formation of six-membered chelates. The metathesis activities of the resulting stable complexes were evaluated, and they unfortunately proved to be less active and *Z*-selective when compared to previously reported cyclometalated catalysts substituted with an *N*-1-adamantyl group. These studies have provided information about how chelating substituents affect the stability, activity, and selectivity of the resulting catalysts. In addition to studying new chelated architectures, two stable dipivalate complexes were isolated. It has been shown that for cyclometalation to occur ruthenium dichloride complexes must first undergo two salt metathesis steps to form a dipivalate intermediate, which then undergoes rapid C−H activation to form a cyclometalated catalyst. However, we have shown here that for some complexes a stable dipivalate complex can form that cannot undergo activation. With these complexes, we were able to probe some of the factors affecting carboxylate-assisted C−H bond activations and determined that flexibility of the N-substituents could prevent cyclometalation.

## EXPERIMENTAL SECTION

**General Information.** All reactions were carried out in dry glassware under an argon atmosphere using standard Schlenk techniques or in a Vacuum Atmospheres glovebox under a nitrogen atmosphere unless otherwise specified. All solvents were purified by passage through solvent purification columns and further degassed by bubbling argon. Hexane was dried over $CaH_2$ and distilled into a dry Schlenk flask and subsequently degassed with argon. THF was purified by passage through solvent purification columns and further degassed with argon. NMR solvents were dried over $CaH_2$ and vacuum transferred to a dry Schlenk flask and subsequently degassed with bubbling argon. $C_6D_6$ was purified by passage through a solvent purification column. $CDCl_3$ was used as received. Potassium *tert*-amyloxide was purchased as a toluene solution and concentrated before use. Dichloro(*o*-isopropoxyphenylmethylene)-(tricyclohexylphosphine)ruthenium [$Ru(PCy_3)(C{=}H\text{-}o\text{-}iPrO\text{-}Ph)Cl_2$] was obtained from Materia, Inc. Other commercially available reagents and silica gel were used as received.



DOI: 10.1021/acs.organomet.5b00185
*Organometallics* XXXX, XXX, XXX−XXX

Purity was established by $^{1}H$ and $^{13}C$ NMR analysis, and identity was demonstrated using high-resolution mass spectrometry. $^{1}H$ and $^{13}C\{^{1}H\}$ NMR spectra were recorded on a Varian 600 MHz spectrometer, a Varian 500 MHz spectrometer, or a Varian 400 MHz spectrometer. High-resolution mass spectra were provided by the California Institute of Technology Mass Spectrometry Facility using a JEOL JMS-600H high-resolution mass spectrometer. X-ray crystallographic data were collected by the California Institute of Technology Beckman Institute X-ray Crystallographic Facility using a Bruker KAPPA APEXII X-ray diffractometer.

*Synthesis of* ***11***. In a glovebox, a 20 mL scintillation vial with a magnetic stir bar was charged with **10** (102 mg, 0.148 mmol, 1 equiv) and NaOPiv (184 mg, 1.48 mmol, 10 equiv). Rigorously deoxygenated THF (ca. 5 mL) and MeOH (ca. 5 mL) were added, and the reaction was heated to 35 °C and stirred for 1 day. During the reaction, the color of the solution changed from green to brown. Upon completion, solvent was removed under reduced pressure. The resulting residue was dissolved in $C_6H_6$, filtered through Celite, and concentrated under reduced pressure. The desired product was purified by column chromatography (5:1 pentane/$Et_2O$ to 1:1 pentane/$Et_2O$ to $Et_2O$), separating away a yellow and green band, yielding a purple solid (13 mg, 12%). $^{1}H$ NMR (600 MHz, $C_6D_6$): $\delta$ 15.06 (s, 1H), 7.54 (dd, $J$ = 7.5, 1.6 Hz, 1 Hz), 7.20 (td, $J$ = 8.0, 1.7 Hz, 1H), 7.13 (t, $J$ = 7.7 Hz, 1H), 7.04 (dd, $J$ = 7.8, 1.5 Hz, 1H), 7.00 (dd, $J$ = 7.6, 1.5 Hz, 1H), 6.88 (td, $J$ = 7.4, 0.8 Hz, 1H), 6.57 (d, $J$ = 8.3 Hz, 1H), 5.02 (dd, $J$ = 9.9, 4.0 Hz, 1H), 4.56 (hept, $J$ = 6.2 Hz, 1H), 3.92 (hept, $J$ = 7.2 Hz, 1H), 3.76 (dt, $J$ = 12.4, 10.2 Hz, 1H), 3.70 (dd, $J$ = 9.9, 2.0 Hz, 1H), 3.34 (td, $J$ = 10.0, 2.4 Hz, 1H), 3.29−3.18 (m, 2H), 2.93 (hept, $J$ = 5.9 Hz, 1H), 1.50 (t, $J$ = 4.2 Hz, 1H), 1.47 (d, $J$ = 6.8 Hz, 3H), 1.40 (d, $J$ = 6.2 Hz, 3H), 1.35 (d, $J$ = 6.1 Hz, 4H), 1.28 (d, $J$ = 6.9 Hz, 4H), 1.24 (d, $J$ = 6.8 Hz, 4H), 1.16 (d, $J$ = 6.9 Hz, 3H), 1.15 (s, 3H), 1.04 (s, 9H), 0.94 (s, 3H), 0.91 (s, 3H), 0.12 (ddd, $J$ = 12.3, 9.5, 3.2 Hz, 1H). $^{13}C\{^{1}H\}$ NMR (126 MHz, $C_6D_6$): $\delta$ 262.65, 219.23, 187.16, 154.52, 148.35, 145.76, 143.07, 137.85, 128.16, 125.62, 123.91, 123.60, 123.04, 122.60, 113.58, 77.29, 73.87, 60.74, 55.21, 52.85, 49.68, 48.95, 47.19, 39.06, 37.44, 29.81, 28.49, 28.21, 27.99, 27.55, 27.07, 26.31, 25.03, 24.49, 23.23, 22.19, 21.88, 21.10, 19.18, 15.71; HRMS-FAB ($m/z$) $[M]^+$ calcd for $C_{40}H_{58}N_2O_3Ru$, 716.3492; found, 716.3508.

*Synthesis of* ***15***. In a glovebox, **S1** (300 mg, 0.836 mmol, 1.1 equiv) and potassium *tert*-amyloxide (96 mg, 0.76 mmol, 1 equiv) were dissolved in hexane (ca. 15 mL) in a 20 mL scintillation vial with a magnetic stir bar. The solution was stirred for 2 h at room temperature and then filtered with a PTFE membrane syringe filter (pore size 0.2 $\mu$m) into a new 20 mL scintillation vial containing $Ru(PCy_3)(C{=}H\text{-}o\text{-}^{i}PrO\text{-}Ph)Cl_2$ (457 mg, 0.76 mmol, 1 equiv) and a magnetic stir bar. The vial was sealed and removed from the glovebox. It was allowed to stir at 65 °C for 4 h. Over the course of the reaction, a green solid precipitated out from the red-brown solution. After cooling to room temperature, the solution was filtered over Celite and the green solid was washed thoroughly with hexane until the washes were colorless. The green solid was collected by dissolving in DCM and concentrating under reduced pressure. The desired product was purified by column chromatography (4:1 pentane/$Et_2O$ to $Et_2O$), yielding a green solid (164 mg, 34%). $^{1}H$ NMR (500 MHz, $CDCl_3$): $\delta$ 16.47 (s, 1H), 7.51 (ddd, $J$ = 8.8, 6.4, 2.6 Hz, 1H), 7.06 (s, 2H), 6.93 (d, $J$ = 8.7 Hz, 1H), 6.90−6.87 (m, 2H), 5.18 (s, 1H), 5.12 (hept, $J$ = 6.1 Hz, 1H), 4.20 (t, $J$ = 8.9 Hz, 2H), 3.94 (t, $J$ = 8.9 Hz, 2H), 2.87 (s, 2H), 2.45 (s, 3H), 2.25 (s, 6H), 2.30−2.17 (m, 4H), 2.08−2.05 (m, 4H), 2.02 (s, 1H), 1.99 (s, 1H), 1.89 (s, 1H), 1.85 (s, 2H), 1.73 (d, $J$ = 6.1 Hz, 6H). $^{13}C\{^{1}H\}$ NMR (126 MHz, $CDCl_3$): $\delta$ 296.61, 211.38, 182.62, 152.47, 144.89, 138.75, 138.63, 138.22, 129.85, 129.71, 123.16, 122.61, 113.13, 74.58, 65.34, 52.43, 49.37, 38.92, 38.20, 34.44, 33.40, 28.07, 27.49, 22.56, 21.32, 18.40. HRMS-FAB ($m/z$): $[M]^+$ calcd for $C_{32}H_{42}Cl_2N_2ORu$, 642.1718; found, 642.1746.

*Synthesis of* ***16***. In a glovebox, a 20 mL scintillation vial with a magnetic stir bar was charged with **15** (140 mg, 0.218 mmol, 1 equiv) and NaOPiv (270 mg, 2.18 mmol, 10 equiv). Rigorously deoxygenated THF (ca. 5 mL) and MeOH (ca. 5 mL) were added, and the reaction was heated to 35 °C and stirred for 1 day. During the reaction, the color of the solution changed from green to brown. Upon completion, solvent was removed under reduced pressure. The resulting residue was dissolved in $C_6H_6$, filtered through Celite, and concentrated under reduced pressure. The residue was dissolved in 5:1 pentane/$Et_2O$ (ca. 3 mL) and let slowly evaporate to yield large blue crystals. The mother liquor was removed and the crystals were washed with pentane (4 × 5 mL) and then $Et_2O$ (2 × 4 mL), yielding pure blue crystals after drying under reduced pressure (19 mg, 13%). The crystals were used for X-ray crystallography to obtain a crystal structure. $^{1}H$ NMR (500 MHz, $C_6D_6$): $\delta$ 14.84 (s, 1H), 7.46 (dd, $J$ = 7.5, 1.6 Hz, 1H), 7.37 (ddd, $J$ = 8.3, 7.4, 1.7 Hz, 1H), 6.89 (td, $J$ = 7.4, 0.8 Hz, 1H), 6.81 (d, $J$ = 6.2 Hz, 2H), 6.69 (d, $J$ = 8.4 Hz, 1H), 4.81 (hept, $J$ = 6.4 Hz, 1H), 3.63−3.43 (m, 1H), 3.39−3.24 (m, 1H), 2.96 (qd, $J$ = 12.0, 11.4, 3.9 Hz, 1H), 2.39−2.36 (m, 1H), 2.33 (s, 3H), 2.31 (td, $J$ = 75.4, 1.9 Hz, 1H), 2.29 (s, 3H), 2.22 (s, 3H), 2.14 (s, 1H), 2.07 (s, 1H), 1.96−1.87 (m, 3H), 1.80 (d, $J$ = 12.1 Hz, 2H), 1.74 (s, 1H), 1.64 (d, $J$ = 6.5 Hz, 3H), 1.54 (d, $J$ = 12.4 Hz, 1H), 1.23 (s, 9H), 1.17 (d, $J$ = 6.2 Hz, 3H), 1.09 (dd, $J$ = 12.4, 2.4 Hz, 1H). $^{13}C\{^{1}H\}$ NMR (126 MHz, $C_6D_6$): $\delta$ 263.52, 219.40, 187.10, 154.02, 144.03, 137.93, 137.14, 136.66, 136.60, 130.05, 129.48, 128.59, 125.79, 123.29, 123.19, 113.77, 80.92, 74.41, 52.17, 50.14, 48.72, 46.04, 39.43, 39.22, 38.67, 38.12, 32.53, 32.37, 31.50, 30.48, 28.50, 21.84, 21.14, 21.03, 18.68. HRMS-FAB ($m/z$)" $[M]^+$ calcd for $C_{37}H_{50}N_2O_3Ru$, 672.2866; found, 672.2868.

*Synthesis of* ***17***. In a glovebox, **S2** (300 mg, 0.75 mmol, 1 equiv) and sodium bis(trimethylsilyl)amide (152 mg, 0.83 mmol, 1.1 equiv) were dissolved in benzene (ca. 10 mL) in a 20 mL scintillation vial with a magnetic stir bar. The solution was stirred for 3 h at room temperature and then filtered with a PTFE membrane syringe filter (pore size 0.2 $\mu$m) into a new 20 mL scintillation vial containing $Ru(PCy_3)(C{=}H\text{-}o\text{-}^{i}PrO\text{-}Ph)Cl_2$ (451 mg, 0.75 mmol, 1.1 equiv) and a magnetic stir bar. The vial was sealed and removed from the glovebox. It was allowed to stir at 50 °C for 4 h. Over the course of the reaction, the solution changed from brown to brown-green. After cooling to room temperature, the solvent was removed under reduced pressure, yielding a green-brown solid. The solid was washed with hexane and filtered over Celite until the washes were colorless. This yielded a green solid. The green solid was collected by dissolving in DCM and concentrating under reduced pressure. The desired product was purified by column chromatography (4:1 pentane/$Et_2O$ to $Et_2O$), yielding a green solid (243 mg, 47%). $^{1}H$ NMR (500 MHz, $C_6D_6$): $\delta$ 16.46 (s, 1H), 7.33 (t, $J$ = 7.7 Hz, 1H), 7.18 (s, 1H), 7.11−7.01 (m, 3H), 6.64 (td, $J$ = 7.5, 0.8 Hz, 1H), 6.38 (d, $J$ = 8.4 Hz, 1H), 5.57 (s, 1H), 4.53 (hept, $J$ = 6.0 Hz, 1H), 3.61−3.53 (m, 2H), 3.52−3.43 (m, 2H), 3.33 (hept, $J$ = 6.8 Hz, 2H), 2.93 (s, 2H), 2.44 (d, $J$ = 12.0 Hz, 2H), 1.94 (t, $J$ = 12.5 Hz, 5H), 1.80 (s, 1H), 1.65 (d, $J$ = 6.1 Hz, 6H), 1.68−1.60 (m, 4H), 1.07 (d, $J$ = 7.0 Hz, 6H), 1.02 (d, $J$ = 6.6 Hz, 6H). $^{13}C\{^{1}H\}$ NMR (126 MHz, $C_6D_6$): $\delta$ 287.50, 213.15, 182.87, 153.18, 149.00, 144.43, 139.01, 129.71, 129.07, 125.17, 122.48, 113.29, 74.69, 66.11, 55.84, 53.33, 49.19, 39.62, 38.59, 34.34, 33.66, 28.52, 28.30, 27.72, 25.78, 24.29, 22.61. HRMS-FAB ($m/z$): $[M]^+$ calcd for $C_{35}H_{48}Cl_2N_2ORu$, 684.2188; found, 684.2179.

*Synthesis of* ***18***. In a glovebox, a 20 mL scintillation vial with a magnetic stir bar was charged with **17** (100 mg, 0.146 mmol, 1 equiv) and NaOPiv (181 mg, 1.46 mmol, 10 equiv). Rigorously deoxygenated THF (ca. 5 mL) and MeOH (ca. 5 mL) were added, and the reaction was heated to 35 °C and stirred for 5 days. During the reaction, the color of the solution changed from green to brown. Upon completion, solvent was removed under reduced pressure. The resulting residue was dissolved in $C_6H_6$, filtered through Celite, and concentrated under reduced pressure. The residue was dissolved in 5:1 pentane/$Et_2O$ (ca. 3 mL) and let slowly evaporate to yield large blue crystals. The mother liquor was removed, and the crystals were washed with pentane (4 × 5 mL) and then $Et_2O$ (2 × 4 mL), yielding pure blue crystals after drying under reduced pressure (10 mg, 10%). The crystals were used for X-ray crystallography to obtain a crystal structure. $^{1}H$ NMR (500 MHz, $C_6D_6$): $\delta$ 15.01 (s, 1H), 7.50 (dd, $J$ = 7.5, 1.6 Hz, 1H), 7.33 (ddd, $J$ = 8.4, 7.4, 1.7 Hz, 1H), 7.19 (t, $J$ = 7.7 Hz, 1H), 7.11 (dd, $J$ = 7.7, 1.6 Hz, 1H), 7.05 (dd, $J$ = 7.6, 1.6 Hz, 1H), 6.88 (td, $J$ = 7.4, 0.7 Hz, 1H), 6.62 (d, $J$ = 8.3 Hz, 1H), 4.72 (hept, $J$ = 6.4 Hz, 1H), 3.98 (hept, $J$ = 6.8 Hz, 1H), 3.69 (ddd, $J$ = 11.9, 10.4, 6.2 Hz, 1H), 3.58 (q, $J$ = 10.5 Hz, 1H), 3.36 (td, $J$ = 10.0, 6.4 Hz, 1H), 3.05−2.93 (m, 2H),



DOI: 10.1021/acs.organomet.5b00185
*Organometallics* XXXX, XXX, XXX−XXX

2.39 (dt, $J$ = 12.5, 2.3 Hz, 1H), 2.29−2.15 (m, 2H), 2.12−2.03 (m, 2H), 1.93−1.85 (m, 2H), 1.83−1.73 (m, 4H), 1.64 (d, $J$ = 6.5 Hz, 3H), 1.59 (d, $J$ = 6.8 Hz, 3H), 1.54−1.46 (m, 1H), 1.44−1.35 (m, 2H), 1.30 (d, $J$ = 2.9 Hz, 3H), 1.29 (d, $J$ = 2.8 Hz, 3H), 1.24 (d, $J$ = 6.9 Hz, 3H), 1.20 (d, $J$ = 6.2 Hz, 3H), 1.08 (s, 9H). $^{13}C\{^1H\}$ NMR (126 MHz, $C_6D_6$): $\delta$ 263.12, 217.48, 167.88, 154.04, 149.08, 147.17, 144.12, 137.59, 128.58, 128.50, 125.80, 124.82, 124.11, 123.21, 123.06, 114.13, 80.54, 74.51, 55.49, 50.04, 48.03, 44.91, 39.36, 39.24, 38.18, 38.06, 34.46, 32.30, 31.30, 30.28, 28.93, 28.81, 28.71, 26.22, 25.31, 23.10, 22.70, 21.90, 21.60 (note: signal at 263.12 ppm detected as cross-peak in HSQC that we are assigning to a benzylidene carbon). HRMS-FAB ($m/z$): $[M + H]^+$ calcd for $C_{40}H_{56}N_2O_3Ru$, 715.3413; found, 715.3383.

*Synthesis of* ***20***. In a glovebox, a 20 mL scintillation vial with a magnetic stir bar was charged with **19** (36 mg, 0.057 mmol, 1 equiv) and NaOPiv (72 mg, 0.57 mmol, 10 equiv). Rigorously deoxygenated THF (ca. 1 mL) and MeOH (ca. 1 mL) were added, and the reaction was heated to 35 °C and stirred for 1 h. During the reaction, the color of the solution changed from green to dark blue. Upon completion, solvent was removed under reduced pressure. The resulting residue was dissolved in $C_6H_6$, filtered through Celite, and concentrated under reduced pressure. The desired product was purified by column chromatography (4:1 pentane/$Et_2O$), yielding the dark blue solid **20** (9 mg, 24%). Crystals suitable for X-ray diffraction were grown from 4:1 pentane/$Et_2O$. $^1H$ NMR (500 MHz, $C_6D_6$): $\delta$ 16.19 (s, 1H), 7.74 (d, $J$ = 7.8 Hz, 1H), 7.33 (t, $J$ = 7.8 Hz, 1H), 6.94 (t, $J$ = 7.3 Hz, 1H), 6.70 (d, $J$ = 8.3 Hz, 1H), 6.44 (s, 1H), 6.37 (s, 1H), 6.31 (d, $J$ = 3.4 Hz, 2H), 4.67 (hept, $J$ = 6.5 Hz, 1H), 4.09 (d, $J$ = 5.2 Hz, 1H), 3.75 (d, $J$ = 5.2 Hz, 1H), 3.28 (s, 3H), 2.62 (s, 3H), 2.43 (s, 3H), 2.21 (s, 3H), 2.04 (s, 3H), 1.95 (s, 3H), 1.92 (s, 3H), 1.50 (s, 9H), 1.43 (d, $J$ = 6.2 Hz, 3H), 1.24 (d, $J$ = 6.2 Hz, 3H). $^{13}C\{^1H\}$ NMR (126 MHz, $C_6D_6$): $\delta$ 263.73, 197.24, 156.15, 145.39, 142.19, 140.40, 136.29, 135.90, 135.21, 135.06, 134.64, 133.81, 128.68, 128.59, 128.42, 128.35, 127.97, 127.71, 125.84, 123.62, 122.68, 113.68, 75.94, 44.54, 31.81, 28.22, 22.75, 22.06, 21.50, 20.86, 20.74, 19.74, 19.47, 18.97, 18.92, 14.31 (note: signal at 263.73 ppm detected as cross-peak in HSQC that we are assigning to a benzylidene carbon); HRMS-FAB ($m/z$): $[M + H]^+ - H_2$ calcd for $C_{36}H_{47}N_2O_3Ru$, 657.2631; found, 657.2620.

*Synthesis of* ***28***. In a glovebox, a 20 mL scintillation vial with a magnetic stir bar was charged with **27** (50 mg, 0.097 mmol, 1 equiv) and NaOPiv (120 mg, 0.97 mmol, 10 equiv). Rigorously deoxygenated THF (ca. 2 mL) and MeOH (ca. 2 mL) were added, and the reaction was stirred at room temperature for 3 h. Upon completion, solvent was removed under reduced pressure. The resulting residue was dissolved in $C_6H_6$, filtered through Celite, and concentrated under reduced pressure, yielding a brown solid. The solid was dissolved in pentane and then stored in a freezer for 1 h. After cooling, a brown solid had precipitated out of solution and was isolated by filtering over Celite. It was then washed with cold pentane (1 mL × 2) and then washed through with room-temperature pentane. Solvent was removed under reduced pressure, yielding a brown solid (28 mg, 42%). A crystal for X-ray crystallography was made by slow evaporation recrystallization in 5:1 pentane/$Et_2O$. $^1H$ NMR (500 MHz, $C_6D_6$): $\delta$ 17.52 (s, 1H), 7.33 (dd, $J$ = 7.5, 1.5 Hz, 1H), 7.05 (ddd, $J$ = 8.9, 7.5, 1.6 Hz, 1H), 6.84−6.76 (m, 3H), 6.47 (d, $J$ = 8.4 Hz, 1H), 4.62 (hept, $J$ = 6.2 Hz, 1H), 2.20 (s, 3H), 2.14 (s, 6H), 1.70 (s, 3H), 1.46 (d, $J$ = 6.3 Hz, 6H), 1.35 (s, 3H), 1.28 (s, 18H). $^{13}C\{^1H\}$ NMR (126 MHz, $C_6D_6$): $\delta$ 251.86, 215.59, 186.23, 155.19, 144.21, 139.51, 139.17, 138.76, 137.42, 129.54, 129.27, 124.03, 122.96, 112.92, 75.54, 39.25, 28.43, 21.49, 21.14, 18.19, 11.97, 11.73. HRMS-FAB ($m/z$): $[M + H]^+$ calcd for $C_{34}H_{48}NO_5RuS$, 684.2297; found, 684.3880.

*Synthesis of* ***29***. In an inert atmosphere glovebox, a vial was charged with imidazolinium salt **S4** (103.1 mg, 0.25 mmol, 1 equiv) and NaO$^t$Bu (24 mg, 0.25 mmol, 1 equiv). Toluene (5 mL) was added, and the mixture was stirred at room temperature for 5 min. Grubbs−Hoveyda 1 (150.3 mg, 0.25 mmol, 1 equiv) was then added, and the mixture was heated to 60 °C for 8 h. The solvent was removed *in vacuo*, and the title compound was purified by silica gel chromatography (5−20% ethyl acetate in hexanes) to give a green-brown solid (161 mg, 67%). $^1H$ NMR (500 MHz, $C_6D_6$): $\delta$ 16.49 (s, 1H), 7.14−7.09 (m, 2H), 6.86−6.81 (m, 2H), 6.70 (td, $J$ = 7.5, 0.8 Hz, 1H), 6.45 (d, $J$ = 8.2 Hz, 1H), 4.86 (dd, $J$ = 12.9, 9.0 Hz, 1H), 4.66 (hept, $J$ = 6.2 Hz, 1H), 4.44 (dd, $J$ = 12.9, 5.1 Hz, 1H), 3.36−3.25 (m, 2H), 3.22−3.08 (m, 2H), 2.66−2.58 (m, 1H), 2.45 (dtd, $J$ = 9.6, 6.3, 1.8 Hz, 1H), 2.30−2.26 (m, 1H), 2.29 (s, 3H), 2.27 (s, 3H), 2.23 (s, 3H), 2.21−2.07 (m, 2H), 1.99−1.95 (m, 1H), 1.94−1.85 (m, 2H), 1.75 (d, $J$ = 6.1 Hz, 3H), 1.71 (d, $J$ = 6.1 Hz, 3H), 1.44 (s, 3H), 1.35 (s, 3H), 1.02 (d, $J$ = 9.6 Hz, 1H). $^{13}C\{^1H\}$ NMR (126 MHz, $C_6D_6$): $\delta$ 288.2, 212.0, 152.8, 144.8, 138.9, 138.6, 138.6, 138.5, 129.9, 129.8, 128.9, 122.4, 122.3, 113.2, 75.0, 58.8, 51.8, 48.5, 45.7, 42.0, 41.3, 39.0, 34.0, 28.4, 26.5, 24.1, 22.4, 22.3, 21.1, 20.2, 18.4, 18.3. HRMS-FAB ($m/z$): $[M]^+$ calcd for $C_{32}H_{44}Cl_2N_2ORu$, 644.1875; found, 644.1889.

*Synthesis of* ***30***. In a glovebox, **29** (98 mg, 0.152 mmol, 1 equiv) was dissolved in THF (1.5 mL). A solution of NaOPiv (188 mg, 1.52 mmol, 10 equiv) in MeOH (1.5 mL) was then added. The vessel was sealed and heated to 50 °C for 7.5 h. A crude aliquot was analyzed by $^1H$ NMR, and full conversion to the bispivalate was observed. The crude mixture was then concentrated *in vacuo*, taken up in ether, and filtered through Celite to give 112 mg (95%) of a dark blue solid. A sample was purified by silica gel column chromatography in the glovebox (25−50% ether in hexanes) to give a bright blue solid. $^1H$ NMR (500 MHz, $C_6D_6$): $\delta$ 18.28 (s, 1H), 7.2−7.15 (m, 1H), 7.05 (ddd, $J$ = 8.2, 7.3, 1.7 Hz, 1H), 6.94 (s, 1H), 6.70 (s, 1H), 6.68 (dd, $J$ = 8.3, 7.4 Hz, 1H), 6.42 (d, $J$ = 8.3 Hz, 1H), 5.19 (t, $J$ = 11.3 Hz, 1H), 4.53 (hept, $J$ = 6.3 Hz, 1H), 3.44−3.38 (m, 2H), 3.28−3.18 (m, 2H), 3.16−3.08 (m, 1H), 2.90 (s, 3H), 2.60−2.50 (m, 2H), 2.48−2.33 (m, 2H), 2.21 (t, $J$ = 5.4 Hz, 1H), 2.14 (s, 3H), 2.13 (s, 3H), 2.15−2.09 (m, 1H), 2.09−2.03 (m, 1H), 1.90−1.81 (m, 1H), 1.75 (s, 3H), 1.61 (d, $J$ = 6.2 Hz, 3H), 1.41 (s, 3H), 1.31 (d, $J$ = 6.3 Hz, 3H), 1.30 (s, 9H), 1.22 (s, 9H), 1.14 (d, $J$ = 9.4 Hz, 1H). $^{13}C\{^1H\}$ NMR (126 MHz, $C_6D_6$): $\delta$ 305.5, 212.1, 187.9, 183.8, 154.3, 144.6, 139.8, 139.1, 138.0, 137.3, 129.7, 129.2, 128.5, 123.2, 122.9, 112.7, 75.2, 57.5, 52.1, 48.4, 46.7, 42.4, 41.1, 39.3, 39.2, 39.1, 34.4, 29.0, 28.8, 28.1, 26.8, 23.8, 21.6, 21.3, 21.0, 19.4, 19.1, 18.6 (note: signal at 305.5 ppm detected as cross-peak in HSQC that we are assigning to a benzylidene carbon). HRMS-FAB ($m/z$): $[M]^+$ calcd for $C_{42}H_{63}N_2O_5Ru]$, 777.3781; found, 777.3800.

**General Cross Metathesis Assay Methods.** Each cross experiment using catalysts **11**, **16**, **18**, and **20** was run in a glovebox at 35 °C with 1 mol % catalyst loading in 3 M THF. Since cross metathesis is an equilibrium reaction, the experiments were left open to the glovebox atmosphere to remove any produced ethylene from the reaction vial. Time points were taken at 1, 2, and 4 h by taking a small aliquot and dissolving in $CDCl_3$. The overall conversion of starting olefin to products was determined by $^1H$ NMR in $CDCl_3$ comparing isomerized product and cross products to the starting material. Additionally, the *Z*-selectivity was determined by comparing the diagnostic peaks for the *E*- and *Z*-olefins of each substrate. Specifically, the diagnostic peaks for *Z*-olefins in $CDCl_3$ are as follows: allyl benzene at 5.78 ppm, 4-pentenol at 5.38−5.19 ppm, and methyl-10-undecenoate at 5.30 ppm. The diagnostic peaks for the *E*-olefins are as follows: allyl benzene at 5.74 ppm, 4-pentenol at 5.45 ppm, and methyl-10-undecenoate at 5.33 ppm. Finally, the ratio of cross product to isomerized material was determined for allyl benzene and 4-pentenol substrates. No isomerized product was noted for the 10-methylundecenoate substrate.

Several experiments were performed to probe the metathesis activity of the dipivalate species **28** and **30**. A simple cross metathesis of allyl benzene with *cis*-1,4-diacetoxy-2-butene at a catalyst loading of 5 mol % catalyst loading in DCM was performed. This reaction was monitored by GC-MS to determine if any new species (i.e., cross products) were formed. After 1 day at 35 °C, no new products were noted by GC, indicating that a simple cross did not occur even to a minimal extent. A simple RCM of diethyl diallylmalonate was performed in deuterated benzene with a catalyst loading of 1 mol % catalyst loading at 50 °C. After 1 day, no ring-closed product was noted by NMR (i.e., no new olefinic peaks were observed). These two reactions, therefore, indicate that this complex does not catalyze RCM or CM reactions.



DOI: 10.1021/acs.organomet.5b00185
*Organometallics* XXXX, XXX, XXX−XXX

## ■ ASSOCIATED CONTENT

### Supporting Information

Experimental details, $^{1}H$ and $^{13}C$ NMR spectra, crystallographic data, and a text file of all computed molecule Cartesian coordinates in a format for convenient visualization. The Supporting Information is available free of charge on the ACS Publications website at DOI: 10.1021/acs.organomet.5b00185.

## ■ AUTHOR INFORMATION


### Corresponding Authors

*E-mail: houk@chem.ucla.edu.
*E-mail: rhg@caltech.edu.

### Author Contributions

§M. B. Herbert and B. A. Suslick contributed equally.


### Notes

The authors declare no competing financial interest.

## ■ ACKNOWLEDGMENTS


Dr. David VanderVelde is thanked for his assistance with NMR characterization and experiments. Lawrence Henling and Dr. Michael K. Takase are acknowledged for X-ray crystallographic analysis. This work was financially supported by the NIH (NIH 5R01GM031332, R.H.G.) and the NSF (CHE-1212767, R.H.G. and CHE-1361104, K.N.H.). The Bruker KAPPA APEXII X-ray diffractometer was purchased via an NSF CRIF:MU award to the California Institute of Technology (CHE-0639094). Materia, Inc. is acknowledged for its generous donation of metathesis catalysts. Calculations were performed on the Hoffman2 cluster at UCLA and the Extreme Science and Engineering Discovery Environment (XSEDE), which is supported by the National Science Foundation (OCI-1053575).


## ■ REFERENCES


(1) (a) Fürstner, A. *Angew. Chem., Int. Ed.* **2000**, *39*, 3012−3043. (b) Trnka, T. M.; Grubbs, R. H. *Acc. Chem. Res.* **2001**, *34*, 18−29. (c) Schrock, R. R. *Chem. Rev.* **2002**, *102*, 145−180. (d) Schrock, R. R.; Hoveyda, A. H. *Angew. Chem., Int. Ed.* **2003**, *42*, 4592−4633. (e) Vougioukalakis, G.; Grubbs, R. H. *Chem. Rev.* **2009**, *110*, 1746−1787. (f) Samojłowicz, C.; Bieniek, M.; Grela, K. *Chem. Rev.* **2009**, *109*, 3708−3742.

(2) Lin, Y. A.; Chalker, J. M.; Davis, B. G. *ChemBioChem* **2009**, *10*, 959−969.

(3) (a) Slugovc, C. *Macromol. Rapid Commun.* **2004**, *25*, 1283−1297. (b) Miyake, G. M.; Piunova, V. A.; Weitekamp, R. A.; Grubbs, R. H. *Angew. Chem., Int. Ed.* **2012**, *51*, 11246−11248. (c) Miyake, G. M.; Weitekamp, R. A.; Piunova, V. A.; Grubbs, R. H. *J. Am. Chem. Soc.* **2012**, *134*, 14249−14254.

(4) Schrodi, Y.; Ung, T.; Vargas, A.; Mkrtumyan, G.; Lee, C. W.; Champagne, T. M.; Pederson, R. L.; Hong, S. H. *Clean: Soil, Air, Water.* **2008**, *36*, 669−673.

(5) (a) Flook, M. M.; Jiang, A. J.; Schrock, R. R.; Müller, P.; Hoveyda, A. H. *J. Am. Chem. Soc.* **2009**, *131*, 7962−7963. (b) Jiang, A. J.; Zhao, Y.; Schrock, R. R.; Hoveyda, A. H. *J. Am. Chem. Soc.* **2009**, *131*, 16630−16631. (c) Yu, M.; Wang, C.; Kyle, A. F.; Jukubec, P.; Dixon, D. J.; Schrock, R. R.; Hoveyda, A. H. *Nature* **2011**, *479*, 88−93. (d) Meek, S. J.; O'Brien, R. V.; Llaveria, J.; Schrock, R. R.; Hoveyda, A. H. *Nature* **2011**, *471*, 461−466. (e) Speed, A. W. H.; Mann, T. J.; O'Brien, R. V.; Schrock, R. R.; Hoveyda, A. H. *J. Am. Chem. Soc.* **2014**, *136*, 16136−16139.

(6) For a study on the mechanism of the C−H activation reaction, see: Cannon, J. S.; Zou, L.; Liu, P.; Lan, Y.; O'Leary, D. J.; Houk, K. N.; Grubbs, R. H. *J. Am. Chem. Soc.* **2014**, *136*, 6733−6743.

(7) For examples of other reported Z-selective ruthenium catalysts, see: (a) Khan, R. K. M.; Torker, S.; Hoveyda, A. H. *J. Am. Chem. Soc.* **2013**, *135*, 10258−10261. (b) Koh, M. J.; Khan, R. K. M.; Torker, S.; Hoveyda, A. H. *Angew. Chem., Int. Ed.* **2014**, *53*, 1968−1972. (c) Khan, R. K. M.; Torker, S.; Hoveyda, A. H. *J. Am. Chem. Soc.* **2014**, *136*, 14337−14340. (d) Occhipinti, G.; Hansen, F. R.; Törnroos, K. W.; Jensen, V. R. *J. Am. Chem. Soc.* **2013**, *135*, 3331−3334. (e) Occhipinti, G.; Koudriavtsev, V.; Tornroos, K. W.; Jensen, V. R. *Dalton Trans.* **2014**, *43*, 11106−11117.

(8) Endo, K.; Herbert, M. B.; Grubbs, R. H. *Organometallics* **2013**, *32*, 5128−5135.

(9) Herbert, M. B.; Lan, Y.; Keitz, B. K.; Liu, P.; Endo, K.; Day, M. W.; Houk, K. N.; Grubbs, R. H. *J. Am. Chem. Soc.* **2012**, *134*, 7861−7866.

(10) Rosebrugh, L. E.; Herbert, M. B.; Marx, V. M.; Keitz, B. K.; Grubbs, R. H. *J. Am. Chem. Soc.* **2013**, *135*, 1276−1279.

(11) MeOH is needed to solubilize the sodium carboxylate starting material.

(12) (a) Liu, P.; Xu, X.; Dong, X.; Keitz, B. K.; Herbert, M. B.; Grubbs, R. H.; Houk, K. N. *J. Am. Chem. Soc.* **2012**, *134*, 1464−1467. (b) Dang, Y.; Wang, Z.-X.; Wang, X. *Organometallics* **2012**, *31*, 7222−7234. (c) Dang, Y.; Wang, Z.-X.; Wang, X. *Organometallics* **2012**, *31*, 8654−8657.

(13) (a) Endo, K.; Grubbs, R. H. *J. Am. Chem. Soc.* **2011**, *133*, 8525−8527. (b) Keitz, B. K.; Endo, K.; Herbert, M. B.; Grubbs, R. H. *J. Am. Chem. Soc.* **2011**, *133*, 9686−9688.

(14) Keitz, B. K.; Endo, K.; Patel, P. R.; Herbert, M. B.; Grubbs, R. H. *J. Am. Chem. Soc.* **2012**, *134*, 693−699.

(15) (a) Herbert, M. B.; Marx, V. M.; Pederson, R. L.; Grubbs, R. H. *Angew. Chem., Int. Ed.* **2013**, *52*, 310−314. (b) Cannon, J. S.; Grubbs, R. H. *Angew. Chem., Int. Ed.* **2013**, *52*, 9001−9004. (c) Quigley, B.; Grubbs, R. H. *Chem. Sci.* **2014**, *5*, 501−506. (d) Mangold, S. L.; O'Leary, D. J.; Grubbs, R. H. *J. Am. Chem. Soc.* **2014**, *136*, 12469−12478.

(16) Marx, V. M.; Herbert, M. B.; Keitz, B. K.; Grubbs, R. H. *J. Am. Chem. Soc.* **2013**, *135*, 94−97.

(17) (a) Hartung, J.; Grubbs, R. H. *J. Am. Chem. Soc.* **2013**, *135*, 10183−10185. (b) Hartung, J.; Grubbs, R. H. *Angew. Chem., Int. Ed.* **2014**, *53*, 3885−3888. (c) Hartung, J.; Dornan, P. K.; Grubbs, R. H. *J. Am. Chem. Soc.* **2014**, *136*, 13029−13037.

(18) Miyazaki, H.; Herbert, M. B.; Liu, P.; Dong, X.; Xu, X.; Keitz, B. K.; Ung, T.; Mkrtumyan, G.; Houk, K. N.; Grubbs, R. H. *J. Am. Chem. Soc.* **2013**, *135*, 5848−5858.

(19) (a) Keitz, B. K.; Fedorov, A.; Grubbs, R. H. *J. Am. Chem. Soc.* **2012**, *134*, 2040−2043. (b) Rosebrugh, L. E.; Marx, V. M.; Keitz, B. K.; Grubbs, R. H. *J. Am. Chem. Soc.* **2013**, *135*, 10032−10035.

(20) (a) These results suggest that oxidative addition of C−H bonds to form these cyclometalated architectures is not occurring.. (b) For mechanistic studies on ruthenium-catalyzed C−H bond activation via the CMD mechanism: Ackermann, L.; Vicente, R.; Althammer, A. *Org. Lett.* **2008**, *10*, 2299−2302.

(21) (a) Lee, C.; Yang, W.; Parr, R. G. *Phys. Rev. B* **1988**, *37*, 785−789. (b) Stephens, P. J.; Devlin, F. J.; Chabalowski, C. F.; Frisch, M. J. *J. Phys. Chem.* **1994**, *98*, 11623−11627.

(22) (a) Zhao, Y.; Truhlar, D. G. *Theor. Chem. Acc.* **2008**, *120*, 215−241. (b) Zhao, Y.; Truhlar, D. G. *Acc. Chem. Res.* **2008**, *41*, 157−167.

(23) Marenich, A. V.; Cramer, C. J.; Truhlar, D. G. *J. Phys. Chem. B* **2009**, *113*, 6378−6396.

(24) Frisch, M. J.; Trucks, G. W.; Schlegel, H. B.; Scuseria, G. E.; Robb, M. A.; Cheeseman, J. R.; Scalmani, G.; Barone, V.; Mennucci, B.; Petersson, G. A.; Nakatsuji, H.; Caricato, M.; Li, X.; Hratchian, H. P.; Izmaylov, A. F.; Bloino, J.; Zheng, G.; Sonnenberg, J. L.; Hada, M.; Ehara, M.; Toyota, K.; Fukuda, R.; Hasegawa, J.; Ishida, M.; Nakajima, T.; Honda, Y.; Kitao, O.; Nakai, H.; Vreven, T.; Montgomery, J. A., Jr.; Peralta, J. E.; Ogliaro, F.; Bearpark, M.; Heyd, J. J.; Brothers, E.; Kudin, K. N.; Staroverov, V. N.; Kobayashi, R.; Normand, J.; Raghavachari, K.; Rendell, A.; Burant, J. C.; Iyengar, S. S.; Tomasi, J.; Cossi, M.; Rega, N.; Millam, M. J.; Klene, M.; Knox, J. E.; Cross, J. B.; Bakken, V.; Adamo, C.; Jaramillo, J.; Gomperts, R.; Stratmann, R. E.; Yazyev, O.; Austin, A. J.; Cammi, R.; Pomelli, C.; Ochterski, J. W.; Martin, R. L.; Morokuma, K.; Zakrzewski, V. G.; Voth, G. A.; Salvador, P.;




DOI: 10.1021/acs.organomet.5b00185
*Organometallics* XXXX, XXX, XXX−XXX

Dannenberg, J. J.; Dapprich, S.; Daniels, A. D.; Farkas, Ö.; Foresman, J. B.; Ortiz, J. V.; Cioslowski, J.; Fox, D. J. *Gaussian 09*, Revision D.01; Gaussian, Inc.: Wallingford, CT, 2009.

(25) For computational studies on the selectivity in palladium-catalyzed carboxylate-assisted C−H activations: (a) Gorelsky, S. I.; Lapointe, D.; Fagnou, K. *J. Am. Chem. Soc.* **2008**, *130*, 10848−10849. (b) Guihaumé, J.; Clot, E.; Eisenstein, O.; Perutz, R. N. *Dalton Trans.* **2010**, *39*, 10510−10519. (c) Gorelsky, S. I.; Lapointe, D.; Fagnou, K. *J. Org. Chem.* **2012**, *77*, 658−668. (d) Petit, A.; Flygare, J.; Miller, A. T.; Winkel, G.; Ess, D. H. *Org. Lett.* **2012**, *14*, 3680−3683.

(26) (a) Rosen, E. L.; Sung, D. H.; Chen, Z.; Lynch, V. M.; Bielawski, C. W. *Organometallics* **2010**, *29*, 250−256. (b) Pazio, A.; Wozniak, K.; Grela, K.; Trzaskowski, B. *Organometallics* **2015**, *34*, 563−570.

(27) *Z*-Content degradation is an issue for this family of cyclometalated catalysts, and current investigations are aimed at elucidating its origins.

(28) Vougiokalakis, G. C.; Grubbs, R. H. *J. Am. Chem. Soc.* **2008**, *130*, 2234−2245.



DOI: 10.1021/acs.organomet.5b00185
*Organometallics* XXXX, XXX, XXX−XXX